medicina

MDPI

Article

Ex Vivo, Nodule-Based Shear Wave Elastography as a Possible Alternative to Intraoperative Frozen Section for Predicting Malignancy in Thyroid Nodules

Süleyman Özkan Aksoy [1,*], Işıl Başara Akın [2], Gökçe Kıran Kazancı [1], Merih Güray Durak [3], Canan Altay [2], Anıl Aysal Ağalar [3], Gökben Yaslı [4] and Ali İbrahim Sevinç [1]

[1] Department of General Surgery, Faculty of Medicine, Dokuz Eylül University, 35340 Izmir, Turkey
[2] Department of Radiology, Faculty of Medicine, Dokuz Eylül University, 35340 Izmir, Turkey
[3] Department of Pathology, Faculty of Medicine, Dokuz Eylül University, 35340 Izmir, Turkey
[4] Department of Public Health, Faculty of Medicine, Izmir Bakircay University, 35340 Izmir, Turkey
* Correspondence: suleyman.aksoy@deu.edu.tr

Abstract

Background and Objectives: Intraoperative frozen section (FS) examination is used to differentiate malignant from benign thyroid nodules but is limited by pathologist dependence, time, and cost. This study evaluated whether ex vivo shear wave elastography (SWE), applied separately to mapped thyroid nodules, could serve as an alternative to FS and investigated the effects of nodule number and tumour size on SWE performance. *Materials and Methods*: A total of 343 thyroid nodules from 100 thyroidectomy patients were mapped and numbered ex vivo. Five two-dimensional SWE measurements were obtained from each nodule using a Philips EPIQ Elite ultrasound system with ElastQ Imaging. Mean, minimum, and maximum stiffness values (kPa) were recorded, and each nodule underwent individual pathological examination. Diagnostic performance was assessed using ROC analysis and the Youden index. Performance was compared according to nodule number (1, 2–3, ≥4) and tumour size (≤10, 11–20, >20 mm). Generalised Estimating Equations (GEE) logistic regression was used to assess independent effects while accounting for within-patient clustering. *Results*: Of 343 nodules, 229 (66.76%) were benign and 114 (33.23%) malignant. Mean SWE was significantly higher in malignant than benign nodules (49.87 ± 21.30 vs. 18.59 ± 5.53 kPa; $p < 0.0001$). ROC analysis yielded an AUC of 0.9396 (95% CI: 0.9110–0.9650). At the 25.40 kPa cutoff, sensitivity, specificity, and accuracy were 84.21%, 90.39%, and 88.33%, respectively. Sensitivity decreased with increasing nodule number (92.30%, 86.11%, 81.53%), whereas tumour size correlated strongly with SWE ($\rho = 0.7807$; $p < 0.0001$). Sensitivity increased from 70.17% for malignant nodules ≤ 10 mm to 100% for those >20 mm. In GEE analysis, nodule number was not independently significant after adjustment for tumour size (OR = 0.93; 95% CI: 0.58–1.47; $p = 0.75$), whereas tumour size remained significant ($p < 0.0001$). *Conclusions*: Ex vivo nodule-based SWE accurately predicts thyroid malignancy. The apparent effect of nodule multiplicity on sensitivity is largely explained by tumour size. SWE may therefore represent a useful adjunct or potential alternative to intraoperative FS, particularly when nodule size is considered.

Keywords: thyroid nodule; shear wave elastography; frozen section; malignancy; TI-RADS; tumor size

Check for updates

Academic Editor: Ioannis Ilias

Received: 25 September 2026
Revised: 25 October 2026
Accepted: 29 October 2026
Published: 31 October 2026

Copyright: © 2026 by the authors. Published by MDPI on behalf of the Lithuanian University of Health Sciences. Licensee MDPI, Basel, Switzerland. This article is an open access article distributed under the terms and conditions of the Creative Commons Attribution (CC BY) license.

1. Introduction

Thyroid nodules represent a frequent occurrence in clinical practice. While the prevalence detected by palpation is approximately 5%, this rate rises to 19–67% with high-resolution ultrasonography and to as high as 50% in autopsy series [1]. While the vast majority of these nodules are benign, the malignancy rate has been documented to range from 5 to 10% across various case series [2].

Fine-needle aspiration biopsy (FNAB) and the Bethesda cytological classification system are the primary tools used to guide the initial clinical decision-making process for thyroid nodules. However, the malignancy risk of nodules falling into cytologically indeterminate categories (Bethesda III and IV) may not be clearly distinguishable [3,4]. In order to reduce the level of uncertainty, the utilisation of an intraoperative frozen section examination has been a customary practice for a considerable period of time, with the objective of determining the necessity for surgical intervention. However, the diagnostic performance of FS is strongly dependent on the experience of the pathologist, the sampling technique, and the histological subtype of the nodule. It has been demonstrated that certain histological subtypes, such as the follicular variant of papillary thyroid carcinoma, are frequently missed by FS, and its routine use is not recommended in recent reviews [5]. In a series of 90 FS cases, Gern et al. reported an overall sensitivity of 75%, and demonstrated that all missed malignancies were the follicular variant of papillary thyroid carcinoma [6]. In a similar vein, Jiang et al. reported the sensitivity of FS in determining the extent of surgery to be 77.61% [7]. Beyond these limitations, FS imposes a substantial cost and time burden, as it requires an experienced pathologist to be present in the operating room [5].

These limitations have increased the need for fast, low-cost methods that are less dependent on the availability of pathologists for the differentiation of malignancy in thyroid nodules. Elastography techniques, which quantify tissue stiffness, have emerged as a promising approach in this field, based on the principle that malignant tissues are generally stiffer than benign tissues [2]. Two primary techniques have been delineated: strain elastography and shear wave elastography (SWE). The latter technique has been shown to offer a distinct advantage over strain elastography by providing a quantitative, comparatively less operator-dependent stiffness value (kilopascals, kPa) through measurement of the propagation speed of shear waves within the tissue [8,9].

A plethora of studies have been published investigating the diagnostic performance of SWE in thyroid nodules. However, marked heterogeneity has been observed among their results. Çakır et al. reported a sensitivity of 73.4% and a specificity of 70.0% using elastosonographic strain index [10]. Bender et al. reported the sensitivity and specificity of ultrasound elastography for detecting carcinoma in a Turkish population as 58.3% and 85.4%, respectively [11]. In their study, Kizilkaya et al. found the sensitivity and specificity of elastography for detecting malignancy to be 67.9% and 75.9%, respectively, and suggested that elastography yielded more reliable results than FNAB [1]. Naleini et al. found high agreement between SWE and FNAB and suggested that SWE could replace FNAB [12]. In contrast, in a systematic review and meta-analysis of 14 studies and 2851 nodules by Nattabi et al., the pooled sensitivity, specificity, and area under the curve (AUC) of quantitative 2D-SWE were 66%, 78%, and 0.851, respectively; the authors emphasised that performance was not as excellent as previously reported [13]. Zhang et al. reported an Area Under the Curve (AUC) of 0.828, using colour-based shear wave elastography (SWE) mapping [14]. The combined use of SWE with TI-RADS classifications has also been investigated; Chambara et al. demonstrated that combining EU-TIRADS with SWE yielded high diagnostic performance in nodules larger than 1 cm, but that sensitivity remained low in cytologically indeterminate nodules [15]. Petersen et al. reported that the incorporation of SWE into the Kwak-TIRADS and EU-TIRADS led to an enhancement in the accuracy of

the diagnostic process. However, the optimal cutoff value exhibited variability across the various series, with a reported value of 18.5 kPa [16]. Gao et al. demonstrated that the incorporation of SWE enhanced the diagnostic accuracy of low- and intermediate-suspicion nodules according to American Thyroid Association (ATA) risk stratification, exhibiting an area under the curve (AUC) of 0.81 as opposed to 0.72 [17]. In a meta-analysis by Qiu et al. focusing on cytologically indeterminate nodules, pooled sensitivity and specificity were 79.2% and 84.5%, respectively [4].

This heterogeneity in the literature may stem from non-standardised measurement protocols, differing cutoff values, and analyses that are generally performed at the patient level rather than the nodule level [2]. The paucity of studies in which each nodule is mapped separately and matched one-to-one with pathology, particularly in cases of multinodular goitre, is a matter of concern. Furthermore, the independent effects of nodule number and tumour size on the diagnostic performance of shear wave elastography (SWE) have not been sufficiently examined. The performance of SWE assessments under ex vivo conditions has been shown to offer a methodological advantage by virtue of the elimination of respiratory and vascular motion artefacts, and by enabling direct comparison of each nodule with pathology. Indeed, Chang et al. demonstrated that ex vivo SWE performed before frozen section provided additional diagnostic value for level VI lymph node assessment in patients with papillary thyroid carcinoma [18].

The objective of this study was to evaluate each thyroid nodule mapped ex vivo in thyroidectomy specimens using SWE, and to compare these findings with pathological results. The primary objective of the study was to ascertain an optimal SWE cutoff value for distinguishing between malignancy and other pathological diagnoses, and to evaluate the feasibility of this method as an alternative or adjunct to intraoperative frozen section analysis. Furthermore, the impact of nodule number (single, 2–3, ≥4 nodules) and tumour size on the diagnostic performance of SWE was examined in detail using statistical methods that account for the dependence among nodules within the same patient.

2. Materials and Methods

2.1. Study Design and Patient Population

The study was designed as a retrospective single-centre, ex vivo diagnostic accuracy study. The study was conducted in the Department of General Surgery, Faculty of Medicine, Dokuz Eylül University, between January 2022 and January 2024. The present study is based on a consecutive series of 100 patients with thyroid nodules on preoperative imaging who underwent thyroidectomy during this period. The study was conducted in accordance with the Declaration of Helsinki and was approved by the Non-Interventional Clinical Research Ethics Committee of Dokuz Eylül University Faculty of Medicine (Protocol No: 2024/13-05; Approval Date: 3 April 2024). Written informed consent was obtained from all subjects.

Patients were eligible for inclusion if they underwent thyroidectomy for one of the following indications: The cases under consideration include the following: (I) cases of malignant or suspicious cytology on fine-needle aspiration biopsy ($n = 58$); (II) cases with imaging features highly suspicious for malignancy ($n = 19$); or (III) cases of hyperthyroidism with coexisting thyroid nodules ($n = 23$). It is notable that no patient had an indication related to tracheal compression. The surgical procedure of choice was a total thyroidectomy, performed in 96 patients, with a lobectomy being carried out on 4 patients. Patients in whom the number and size of nodules could not be clearly assessed on radiological examination were excluded from the study. In consideration of the aforementioned selection criteria, the study population exhibited a higher prevalence of malignancy in comparison with unselected thyroid nodule populations and with thyroidectomies performed

for all indications. This observation should be taken into account when interpreting the predictive values reported below.

2.2. Ex Vivo Ultrasonography and Shear Wave Elastography Protocol

All B-mode ultrasonographic and elastographic assessments were performed ex vivo on the excised thyroidectomy specimen using a Philips EPIQ Elite ultrasound system (Philips Healthcare, Bothell, WA, USA) equipped with an eL18-4 linear probe. A sufficient quantity of air bubble-free ultrasound gel was applied over each target area to ensure optimal acoustic transmission. The thyroid nodules present in each patient were meticulously mapped and individually numbered ex vivo (343 nodules in total). Each numbered nodule was evaluated with a standard B-mode examination, covering both axial dimensions and additional features. This was followed by a 2D-SWE examination using the ElastQ Imaging module.

During the acquisition of SWE data, the system's integrated reliability mapping tool, designated as the Confidence Map, was engaged, and data collection was confined to homogeneous tissue regions exhibiting high propagation reliability (colour-coded green). Quantitative elasticity values were obtained using regions of interest (ROIs) placed over the visibly stiffest area of each thyroid nodule. A square ROI of 3 × 3 mm was used, and care was taken to exclude the nodule margins and surrounding parenchyma. All measurements were performed by two radiologists in consensus, and the five measurements of each nodule were obtained from three to four different locations within the nodule. Five distinct measurements were obtained from each nodule, and the mean, minimum, and maximum stiffness values were documented and expressed in kilopascals (kPa). The arithmetic mean of the five measurements was used as the primary elastographic parameter for each nodule.

Each nodule was submitted for pathological sampling after ex vivo imaging and matched with its final pathology result. The pathological examination was accepted as the reference standard, and nodules were classified as benign or malignant accordingly.

2.3. Subgroup Definitions

In order to evaluate the effect of nodule number on SWE performance, patients were divided into three groups according to the number of nodules present: single nodule ($n = 13$ patients), 2–3 nodules ($n = 39$ patients), and ≥4 nodules ($n = 48$ patients). In order to evaluate the effect of tumour size, nodules which were pathologically confirmed as malignant were divided into three groups according to size: ≤10 mm ($n = 57$), 11–20 mm ($n = 24$), and >20 mm ($n = 33$).

2.4. Statistical Analysis

Statistical analyses were conducted at both the patient level and the nodule level. The descriptive statistics for continuous variables are presented as the mean ± standard deviation (SD) and median (first–third quartile; Q_1–Q_3), and for categorical variables, these are presented as number (n) and percentage (%). The normality of continuous variables was assessed using the Shapiro–Wilk test. Age was normally distributed ($p = 0.11$), whereas SWE values (benign nodules, $p = 0.017$; malignant nodules, $p < 0.001$) and tumour size ($p < 0.001$) were not; non-parametric tests were therefore used for comparisons. Both mean ± SD and median (Q_1–Q_3) are reported, the former to allow comparison with previous SWE studies, most of which report mean values, and the latter as the appropriate summary for non-normally distributed data.

The Mann–Whitney U test was employed to compare the SWE values (minimum, mean, maximum) of benign and malignant nodules, given the non-normal distribution of the data. The diagnostic performance of SWE in differentiating benign from malignant nodules was evaluated with receiver operating characteristic (ROC) curve analysis, using the mean of the

five measurements as the primary diagnostic variable. The optimal SWE cutoff value was determined using the Youden index (sensitivity + specificity − 1). The values of sensitivity, specificity, positive predictive value (PPV), negative predictive value (NPV), and overall accuracy were calculated for this value, together with 95% confidence intervals.

For the nodule-number subgroups, the single SWE cutoff value derived from the overall ROC analysis was applied to all groups, and sensitivity and specificity were calculated for each group; AUC values were additionally determined for the appropriate groups. As all 13 nodules in the single-nodule group were malignant, a benign comparison group was not available in this subgroup. Consequently, specificity and AUC could not be calculated.

The relationship between tumour size and SWE values was evaluated using Pearson and Spearman correlation analyses in nodules that were confirmed as malignant. The Kruskal–Wallis test was utilised to compare SWE distributions across tumour-size groups, and Pearson's chi-square (χ^2) test was employed to evaluate the relationship between tumour-size category and positivity according to the SWE cutoff value.

In order to ascertain whether the effect of nodule number on the accurate detection of malignant nodules by SWE was independent of tumour size, a logistic regression analysis using generalised estimating equations (GEE) was performed, restricted to nodules that were pathologically confirmed as malignant. The dependent variable was defined as a binary outcome, corresponding to whether the nodule's SWE value exceeded the determined cutoff value (true positive detection). Given the potential for multiple nodules to occur within a single patient, a within-patient correlation among nodules was incorporated into the model through the implementation of a patient-identity-based clustering method. The model utilised a binomial distribution, a logit link function, an exchangeable working correlation structure, and robust standard errors. The nodule number was entered as a continuous variable, while the tumour size was entered as a continuous variable, with an increase of 10 mm per unit. The results of the regression analysis are reported as odds ratio (OR), 95% confidence interval (CI), and *p*-value. Because the number of false-negative observations was small and SWE positivity was nearly complete in larger tumours, model diagnostics (number of events, events per variable, cluster structure and the estimated working correlation) were examined, and the following sensitivity analyses were performed: (I) GEE with an independence working correlation structure; (II) tumour size modelled as log2-transformed size (per doubling) and dichotomised at 10 mm; (III) nodule number modelled as a categorical variable (1, 2–3, ≥4); (IV) Firth penalised logistic regression, which reduces small-sample bias in the presence of separation, with 95% CIs additionally estimated by patient-level cluster bootstrap (1000 resamples); and (V) patient-level cluster bootstrap of the GEE model (1000 resamples).

It is imperative to note that all statistical tests were two-tailed, and a *p*-value less than 0.05 was considered to be statistically significant. Descriptive and non-parametric analyses were conducted utilising IBM SPSS Statistics version 26.0, while multivariable models were verified employing Python statsmodels version 0.14.6; sensitivity analyses were performed using statsmodels version 0.15.0.

3. Results

3.1. Patient Characteristics

A total of 100 patients were included in the study. The mean age of the patients was 50.8 ± 14.2 years (median 54.0 years; IQR 41.0–61.0). The demographic and clinical characteristics of the patients are summarised in Table 1. The presence of comorbidity was identified in 39 patients. The surgical indication was identified as cytological/biopsy suspicion in 58 patients, radiological suspicion in 19 patients, and hyperthyroidism in 23 patients. Malignancy was identified on final pathology in 18 of the 19 patients operated

on for radiological suspicion, in all 58 patients operated on for cytological/biopsy suspicion, and in 15 of the 23 patients operated on for hyperthyroidism. The surgical procedure of choice was a total thyroidectomy, performed in 96 patients, with a lobectomy being carried out on 4 patients. The radiological assessment yielded a classification of 82 patients as malignant/suspicious and 18 as benign. Multiple nodules were identified in 86 patients, while a single nodule was found in 14 patients. The distribution of nodule number was as follows: 1 nodule ($n = 13$), 2 nodules ($n = 17$), 3 nodules ($n = 22$), 4 nodules ($n = 22$), 5 nodules ($n = 14$), and 6 nodules ($n = 12$). The distribution by TI-RADS category was as follows: TI-RADS 2 ($n = 10$), 3 ($n = 20$), 4 ($n = 39$), and 5 ($n = 31$).

Table 1. Demographic and clinical characteristics of the patients ($n = 100$).

Characteristic	Result
Age, years	
Mean ± SD	50.8 ± 14.2
Median (Q_1–Q_3)	54.0 (41.0–61.0)
Surgical indication, *n* (%)	
Radiological suspicion	19 (19%)
Biopsy suspicion	58 (58%)
Hyperthyroidism	23 (23%)
Operation, *n* (%)	
Total thyroidectomy	96 (96%)
Lobectomy	4 (4%)
Radiological assessment, *n* (%)	
Benign	18 (18%)
Malignant/suspicious	82 (82%)
Nodule number, *n* (%)	
1	13 (13%)
2	17 (17%)
3	22 (22%)
4	22 (22%)
5	14 (14%)
6	12 (12%)
TI-RADS, *n* (%)	
2	10 (10%)
3	20 (20%)
4	39 (39%)
5	31 (31%)
Tumor type, *n* (%)	
Papillary	87 (87%)
Follicular	2 (2%)
Hürthle cell	1 (1%)
Medullary	1 (1%)
Benign	9 (9%)
Pathological tumor size *, mm	
Mean ± SD	18.56 ± 14.10;
Median (Q_1–Q_3)	13.00 (8.50–26.50)

Table 1. *Cont.*

Characteristic	Result
T-stage *, *n* (%)	
T1a	37 (40.7%)
T1b	21 (23.1%)
T2	22 (24.2%)
T3	11 (12.1%)
Family history, *n* (%)	
Absent	95 (95%)
Present	5 (5%)

* Pathological tumor size and T-stage were recorded in 91 patients. Continuous variables are presented as mean ± SD and median (IQR).

On final pathology, the tumour type was papillary in 87 patients, follicular in 2, Hürthle cell in 1, and medullary carcinoma in 1, with 9 patients found to be benign. The data set included pathological tumour size and T-stage information for 91 patients, with a mean tumour size of 18.56 ± 14.10 mm (median 13.00 mm, interquartile range 8.50–26.50). The distribution of T-stage was as follows: T1a ($n = 37$), T1b ($n = 21$), T2 ($n = 22$), T3a ($n = 10$), and T3b ($n = 1$). Lymph node invasion was observed in two patients (in incidentally excised lymph nodes within the thyroidectomy specimen), neural invasion in three patients, and capsular invasion in fifty-nine patients. The medical records of the patients revealed a history of radiotherapy in two cases, and a family history in five cases.

3.2. Nodule-Level SWE Values: A Comparative Analysis of Benign and Malignant Thyroid Nodules

A total of 343 thyroid nodules were evaluated in this study; of these, 229 (66.76%) were found to be benign and 114 (33.23%) were malignant. The minimum, mean, and maximum SWE values of benign and malignant nodules are presented in Table 2. SWE values of malignant nodules were found to be significantly higher than those of benign nodules for each of the minimum, mean, and maximum measurements (Mann–Whitney U test, $p < 0.0001$ for each). The mean SWE value was 18.59 ± 5.53 kPa (median 18.20; IQR 14.80–22.00) in benign nodules, compared with 49.87 ± 21.30 kPa (median 49.50; IQR 29.85–67.35) in malignant nodules.

Table 2. Comparison of SWE values of benign and malignant thyroid nodules (100 patients, 343 nodules; SWE: mean of 5 measurements per nodule).

Variable Mean ± SD Median (Q_1–Q_3)	Benign ($n = 229$)	Malignant ($n = 114$)	p *
SWE minimum, kPa	12.31 ± 4.93 11.0 (11.0–12.0)	40.99 ± 20.84 40.50 (22.00–55.00)	<0.0001
SWE mean, kPa	18.59 ± 5.53 18.20 (14.80–22.00)	49.87 ± 21.30 49.50 (29.85–67.35)	<0.0001
SWE maximum, kPa	25.51 ± 7.07 23.00 (21.00–32.00)	59.49 ± 28.50 56.50 (37.00–77.00)	<0.0001

* Mann–Whitney U test.

3.3. Diagnostic Performance of SWE

The diagnostic performance of the mean SWE value in differentiating benign from malignant thyroid nodules was evaluated through ROC curve analysis. The area under the curve (AUC) was calculated as 0.9396 (95% CI: 0.9110–0.9650) (see Figure 1). The

optimal SWE cutoff value determined by the Youden index was 25.40 kPa; at this threshold, sensitivity was 84.21% (95% CI: 76.41–89.77), specificity was 90.39% (95% CI: 85.88–93.56), positive predictive value (PPV) was 81.35%, negative predictive value (NPV) was 92.00%, and overall accuracy was 88.33% (Table 3).

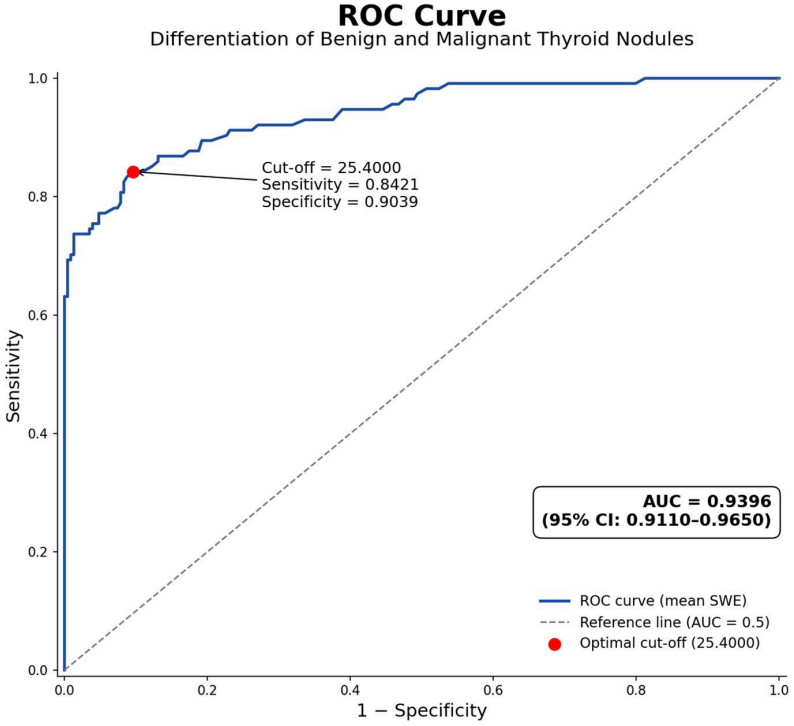


Figure 1. ROC curve showing the diagnostic performance of the mean shear wave elastography (SWE) value in differentiating benign from malignant thyroid nodules. Pathological examination was accepted as the reference standard. In the ROC analysis of a total of 343 nodules (229 benign, 114 malignant), the AUC was 0.9396 (95% CI: 0.9110-0.9650). The optimal SWE cutoff value according to the Youden index was 25.40, at which sensitivity was 84.21% and specificity was 90.39%.

Table 3. Overall nodule-level SWE diagnostic performance results.

Variable	Result
Total nodules, *n*	343
Benign nodules, *n* (%)	229 (66.76)
Malignant nodules, *n* (%)	114 (33.23)
Mean SWE in benign nodules, kPa Mean ± SD	18.59 ± 5.53
Mean SWE in malignant nodules, kPa Mean ± SD	49.87 ± 21.30
ROC AUC (95% CI)	0.9396 (0.9110–0.9650)
Optimal SWE cutoff (Youden), kPa	25.40
Sensitivity, % (95% CI)	84.21 (76.41–89.77)
Specificity, % (95% CI)	90.39 (85.88–93.56)
PPV, %	81.35
NPV, %	92.00
Accuracy, %	88.33

3.4. Effect of Nodule Number on SWE Performance

The diagnostic performance of SWE in subgroups formed according to nodule number is presented in Table 4. In the single-nodule group (n = 13 patients, 13 nodules, all malignant), the proportion of nodules above the 25.40 kPa cutoff (sensitivity) was 92.30%. As there was no benign comparison nodule in this group, specificity and AUC could not be calculated. In the 2–3 nodule group (n = 39 patients, 101 nodules, 36 malignant), the sensitivity was 86.11%, the specificity was 87.69%, and the AUC was 0.93; in the ≥4 nodule group (n = 48 patients, 229 nodules, 65 malignant), the sensitivity was 81.53%, the specificity was 91.46%, and the AUC was 0.93.

Table 4. SWE diagnostic performance according to nodule number.

Number of Nodules	Patients, *n*	Nodules, *n*	Malignant, *n*	Sensitivity (%)	Specificity (%)	AUC
1	13	13	13	92.30	Not applicable *	Not applicable *
2–3	39	101	36	86.11	87.69	0.93
≥4	48	229	65	81.53	91.46	0.93

* Because all 13 nodules in the single-nodule group were malignant, there was no benign comparison group; specificity and AUC could therefore not be calculated. The same 25.40 kPa SWE cutoff value was applied across all groups.

Although a gradual decrease in sensitivity calculated at the fixed 25.40 kPa cutoff was observed as nodule number increased (92.30% → 86.11% → 81.53%), the AUC values of the 2–3 and ≥4 nodule groups were quite close to one another and high (0.93 for both). This finding suggests that the capacity of SWE to differentiate malignant from benign nodules (AUC, a threshold-independent metric) is preserved independently of nodule number. However, a single fixed cutoff value derived from the entire cohort (25.40 kPa) may lead to false-negative results in some nodules of patients with multiple nodules, particularly smaller malignant nodules. This distinction is addressed further below together with the tumor-size findings.

3.5. Relationship Between Tumor Size and SWE

The present analysis was performed on 114 nodules that were subsequently confirmed to be malignant on a pathological basis. The mean tumour size was 16.60 ± 13.76 mm (median 10.50 mm, range 2–55 mm). A robust, affirmative, and statistically significant relationship was identified between tumour size and mean SWE value (see Table 5). Pearson's rho = 0.6854 ($p < 0.0001$); Spearman's ρ = 0.7807 ($p < 0.0001$). The higher value of the Spearman coefficient relative to the Pearson coefficient suggests that the relationship may not be entirely linear.

Table 5. Relationship between tumor size and SWE in malignant nodules.

Analysis	Coefficient	*p*
Pearson correlation	r = 0.6854	<0.0001
Spearman correlation	ρ = 0.7807	<0.0001

The analysis was performed on the 114 nodules pathologically confirmed as malignant (relationship between tumor size and mean SWE value).

The malignant nodules were then divided into three groups according to tumour size: ≤10 mm (n = 57), 11–20 mm (n = 24), and >20 mm (n = 33). The mean shear wave elasticity (SWE) values were found to be 35.80 ± 15.64 kPa, 55.92 ± 14.04 kPa, and 69.77 ± 15.60 kPa, respectively. A statistically significant difference was found between the

groups (Kruskal–Wallis H = 53.60, $p < 0.0001$). Within the same groups, the sensitivity of the 25.40 kPa cutoff value, derived from the overall ROC analysis, was 70.17% in nodules measuring ≤10 mm, 95.83% in nodules measuring 11–20 mm, and 100.00% in nodules measuring >20 mm. The relationship between tumor size category and positivity according to the cutoff value was statistically significant ($\chi^2 = 17.07$, $p = 0.0002$) (Table 6).

Table 6. SWE values and sensitivity according to tumor-size groups.

Tumor Size	Malignant Nodules, *n*	SWE (kPa) Mean ± SD	SWE Median (Q_1–Q_3)	Sensitivity (%)
≤10 mm	57	35.80 ± 15.64	30.00 (24.34–49.60)	70.17
11–20 mm	24	55.92 ± 14.04	58.10 (45.35–65.22)	95.83
>20 mm	33	69.77 ± 15.60	68.78 (62.40–84.00)	100.00

Between-group SWE comparison: Kruskal–Wallis H = 53.5987, $p < 0.0001$. Relationship between size group and SWE positivity according to the 25.40 kPa cutoff: $\chi^2 = 17.0703$, $p = 0.0002$.

In summary, as the size of the tumour increases, so does the stiffness value measured by elastography, and the sensitivity of SWE for detecting malignant nodules rises; however, sensitivity is notably reduced in malignant nodules with a diameter of ≤10 mm.

3.6. Assessment of the Independent Effects of Nodule Number and Tumor Size (GEE Logistic Regression)

In order to distinguish between the apparent effect of nodule number on SWE performance being due to the tendency of malignant nodules to be smaller in patients with multiple nodules, and nodule number itself being the cause, a GEE logistic regression analysis was performed that accounted for clustering among nodules within the same patient (see Table 7). The model was constructed using only those malignant nodules for which a pathological confirmation was obtained, with the dependent variable defined as the SWE value exceeding the 25.40 kPa cutoff (true positive detection). When the size of the tumour was included in the model, the number of nodules (per 1-nodule increase) had no statistically significant independent effect on the true positive detection by SWE (OR = 0.9260, 95% CI: 0.58–1.47; $p = 0.7463$). Conversely, the association between tumour size and the probability of true positive detection by SWE was found to be statistically significant (OR = 100.0571, 95% CI: 10.47–955.99; $p < 0.0001$). Expressed per 1 mm increase, this corresponds to an OR of 1.58 (95% CI: 1.26–1.99). The very wide confidence interval of the per 10 mm estimate reflects the small number of false-negative observations ($n = 18$), 17 of which occurred in nodules ≤10 mm, and the near-complete separation of the outcome at larger tumour sizes (all 33 malignant nodules >20 mm were SWE-positive). This estimate should therefore be interpreted as indicating the direction and strength of the association rather than a precise effect size.

The following is a model diagnostics and sensitivity analysis. The model incorporated 114 malignant nodules from 91 patients (71 patients with one, 17 with two and 3 with three malignant nodules) and 18 false-negative observations, corresponding to 9 events per variable. The estimated exchangeable working correlation was found to be close to zero ($\alpha \approx -0.06$), indicating minimal within-patient dependence. The results of the sensitivity analyses are presented in Table 8. In all specifications, nodule number had no significant independent effect (all $p \geq 0.22$), whereas tumour size remained significantly associated

with true positive detection (all $p \leq 0.0024$). When the size of the tumour was modelled on a logarithmic scale, it was found that each doubling of tumour size was associated with an odds ratio (OR) of 8.65 (95% confidence interval [CI]: 3.50–21.38). Furthermore, it was determined that nodules measuring ≤10 mm had markedly lower odds of detection in comparison to larger nodules (OR = 0.04; 95% CI: 0.005–0.32). Firth penalised regression yielded a smaller per 10 mm estimate (odds ratio [OR] = 72.26; 95% confidence interval [CI] = 6.69–780.00). In the cluster bootstrap of the GEE model, 138 of 1000 resamples failed to converge or yielded non-finite estimates, and the bootstrap confidence interval for tumour size was found to be very wide (19.33–15,054.39). When considered as a whole, these findings indicate that the direction and statistical significance of the tumour-size effect, and the absence of an independent nodule-number effect, are robust to model specification. By contrast, the magnitude of the per 10 mm estimate is unstable owing to near-complete separation and should not be interpreted as a precise effect size. Sensitivity analyses consistently supported a positive association between tumour size and SWE positivity. However, the wide confidence intervals and unsuccessful GEE bootstrap fits indicate substantial uncertainty in the effect magnitude. No statistically significant association with nodule number was detected.

Table 7. GEE logistic regression results evaluating the effects of nodule number and tumor size on true positive detection by SWE.

Variable	β	OR	95% Confidence Interval	*p*
Nodule number (per 1-nodule increase)	−0.0769	0.9260	0.58–1.47	0.7463
Tumor size (per 10 mm increase)	4.6057	100.0571	10.47–955.99	<0.0001

The dependent variable was defined as SWE ≥ 25.40 kPa (true positive detection) in nodules pathologically confirmed as malignant. Correlation among multiple nodules belonging to the same patient was accounted for using a GEE model (exchangeable correlation structure, robust standard errors). OR: Odds Ratio; ; SWE: Shear Wave Elastography.

Table 8. Sensitivity analyses of the association of nodule number and tumour size with true positive detection by SWE in malignant nodules ($n = 114$).

Model	Nodule Number, OR (95% CI); *p*	Tumour Size, OR (95% CI); *p*
GEE, independence working correlation	0.99 (0.64–1.52); 0.97	111.51 (9.27–1340.60) per 10 mm; 0.0002
GEE, log2-transformed tumour size	1.03 (0.67–1.58); 0.90	8.65 (3.50–21.38) per doubling; <0.0001
GEE, tumour size dichotomised	0.80 (0.57–1.14); 0.22	0.04 (0.005–0.32) for ≤10 vs. >10 mm; 0.0024
GEE, nodule number categorical (reference: 1 nodule)	2–3: 1.34 (0.07–24.82); 0.84 ≥4: 1.13 (0.06–20.64); 0.93	116.47 (10.63–1276.55) per 10 mm; 0.0001
Firth penalised logistic regression	0.99 (0.66–1.47); 0.95	72.26 (6.69–780.00) per 10 mm; 0.0004
Firth regression, cluster bootstrap 95% CI (1000/1000 resamples)	0.66–1.64	13.34–2360.11 per 10 mm
GEE, cluster bootstrap 95% CI (862/1000 resamples converged)	0.52–2.20	19.33–15,054.39 per 10 mm

Dependent variable: SWE ≥ 25.40 kPa (true positive detection) in pathologically confirmed malignant nodules. GEE models used robust standard errors with patient-level clustering; unless otherwise stated, an exchangeable working correlation structure and tumour size per 10 mm increase were used. Cluster bootstrap CIs were obtained by resampling patients with replacement (percentile method). GEE: generalised estimating equations; OR: odds ratio; CI: confidence interval.

The findings demonstrate that the decline in fixed-threshold sensitivity observed as nodule number increases is a confounding effect arising from the tendency of malignant

nodules to be comparatively smaller in patients with multiple nodules, rather than from nodule number itself. In other words, once the size of the tumour has been controlled for, the number of nodules has no independent adverse effect on SWE performance.

4. Discussion

In the present study, the 343 thyroid nodules mapped ex vivo in thyroidectomy specimens were subject to separate evaluation by SWE, and then compared with pathology. The mean SWE value was found to differentiate benign from malignant nodules with high accuracy (AUC 0.94); at the 25.40 kPa cutoff determined by the Youden index, the sensitivity was 84.2% and the specificity was 90.4%. This performance is considerably higher than that reported in most in vivo SWE studies in the literature. For instance, in the meta-analysis by Nattabi et al., pooled sensitivity, specificity, and AUC were 66%, 78%, and 0.851, respectively [13]. Individual elastography studies have reported sensitivities of 58–80% and specificities of 49–85% [1,10,11,16], and an AUC of 0.828 was reported for colour SWE scoring [14].

When interpreting these results, it should be noted that sensitivity and specificity are largely independent of disease prevalence, whereas positive and negative predictive values are not. Although the patient-level malignancy rate in our selected surgical cohort was high (91%), all diagnostic analyses were performed at the nodule level, where the prevalence of malignancy was 33.2% (114/343), because most patients harboured multiple benign nodules in addition to the malignant one. Even so, this prevalence exceeds the 5–10% malignancy rate reported in routine thyroid nodule assessment [2]. Applying the sensitivity and specificity observed in this study, the expected PPV and NPV would be approximately 68.7% and 95.8% at a malignancy prevalence of 20%, 49.3% and 98.1% at 10%, and 31.6% and 99.1% at 5%. Thus, the PPV of 81.35% observed in our cohort cannot be directly extrapolated to lower-prevalence populations, in which SWE may be more useful for ruling out than for confirming malignancy. These hypothetical calculations assume that sensitivity and specificity remain unchanged across populations. They illustrate the influence of prevalence on predictive values but do not establish the clinical rule-out performance of SWE in routine thyroid nodule assessment.

The higher performance observed in this study may be explained by several factors. Firstly, ex vivo assessment may have increased measurement reproducibility by eliminating artefacts related to respiratory motion, vascular pulsation, and patient movement. Secondly, the discrete mapping and numbering of each nodule on the surgical specimen permitted direct and precise matching of the measurement to the corresponding pathology result, thereby eliminating the uncertainty commonly encountered in patient-level analyses due to mismatching. Thirdly, the placement of the ROI over the visibly stiffest area of the nodule, in conjunction with the utilisation of the system's Confidence Map tool for reliability mapping, has the potential to enhance the accuracy of the measurement. However, it should be noted that potential variations in tissue perfusion, temperature, and preload occurring under ex vivo conditions may result in differences between the measured stiffness values and those obtained in vivo. This issue is further elaborated upon in the Limitations section.

Our findings suggest that SWE may be a potential adjunct or alternative to intraoperative FS. FS performance depends strongly on the pathologist's experience and remains limited in Bethesda III–IV nodules, with reported sensitivities of 75–78% [5–7]. The sensitivity and specificity observed in this study (84.2% and 90.4%) are comparable to, or exceed, these values. Moreover, SWE does not require an experienced pathologist in the operating room, is relatively inexpensive and provides results within minutes. However, as the two methods were not compared on the same nodules, the claim that SWE could replace FS should be regarded with caution until it is supported by direct comparative studies.

A further key finding is that the apparent adverse effect of nodule number on SWE performance was confounded by tumour size. Although sensitivity at the fixed cutoff decreased as nodule number increased (92.30%, 86.11% and 81.53%), the AUC values of the 2–3 and ≥4 nodule groups were identical (0.93). As AUC is a threshold-independent measure, this indicates that the discriminative capacity of SWE is preserved irrespective of nodule number, and that the decline in sensitivity reflects the fact that a single cohort-derived cutoff is not optimal for every subgroup. Furthermore, in the GEE analysis accounting for within-patient clustering, nodule number had no independent effect on true positive detection once tumour size was controlled for (OR = 0.93, 95% CI: 0.58–1.47; $p = 0.75$), whereas tumour size remained strongly associated (OR = 100.06 per 10 mm, equivalent to 1.58 per 1 mm; $p < 0.0001$), a finding that was robust across all sensitivity analyses. The smaller size of malignant nodules in patients with multiple nodules therefore underlies the observed decline in sensitivity. Clinically, rather than questioning the reliability of SWE in multinodular goitre, clinicians should be particularly attentive to small (≤10 mm) malignant nodules and should use complementary diagnostic methods when necessary.

Indeed, a robust, positive correlation was identified between tumour size and SWE stiffness value (Spearman $\rho = 0.78$, $p < 0.0001$). This correlation can be attributed to the increasing fibrosis, desmoplastic stromal reaction, and cellular density that accompany the growth of malignant tumours. The size-group analysis demonstrated that SWE sensitivity was significantly diminished in malignant nodules measuring ≤10 mm (70.17%), reaching 95.83% in nodules measuring 11–20 mm, and culminating at 100.00% in nodules > 20 mm. This finding is consistent with the literature; technical factors such as the difficulty of the ROI fully representing small nodules, partial volume effect, and contribution of surrounding tissue to the measurement may limit the sensitivity of SWE in small malignant nodules [8,9]. Consequently, particularly in nodules measuring 1 cm or less, the interpretation of SWE results should be informed by a combination of other imaging and cytological findings, as opposed to a standalone approach.

The clinical consequences of false-negative SWE results in small nodules merit specific consideration. Of the 18 false-negative malignant nodules in the entire cohort, 17 measured ≤10 mm (17 of 57 nodules in this size group, compared with 1 of 24 in the 11–20 mm group and none of the 33 nodules > 20 mm). All false-negative nodules occurred in patients with papillary carcinoma, and 12 of the 17 false-negative nodules ≤ 10 mm measured ≤5 mm. Such papillary microcarcinomas generally carry a low risk of recurrence and disease-specific mortality; current guidelines consider lobectomy sufficient for unifocal, intrathyroidal, low-risk carcinomas smaller than 1 cm without clinical evidence of nodal metastasis or extrathyroidal extension, and active surveillance is an accepted alternative in selected patients [19]. In this setting, a false-negative SWE result in a ≤10 mm nodule would rarely, on its own, lead to inadequate treatment of clinically significant disease. However, missing a small malignant focus could lead to under-recognition of multifocal or bilateral disease, which may be relevant when deciding between lobectomy and total thyroidectomy. Therefore, in its current form, SWE should not be used as the sole basis for intraoperative decisions in nodules ≤ 10 mm: a positive result may support a decision to extend surgery, but a negative result in a small nodule should not be regarded as evidence of benignity, and frozen section or final histopathology should be relied upon when the result would alter the extent of surgery. A lower, size-specific cutoff value might improve sensitivity in small nodules at the expense of specificity; this should be evaluated in larger cohorts. Neither a positive nor a negative SWE result should independently determine the extent of surgery, particularly in nodules ≤ 10 mm.

The findings of this study are consistent with those of other studies in the literature that have evaluated the combination of TI-RADS and SWE. Chambara et al. and Petersen et al.

reported that the incorporation of SWE into the TI-RADS classification system enhanced diagnostic accuracy, though performance exhibited variability in relation to nodule size and cytological indeterminacy [15,16]. In a similar vein, Gao et al. demonstrated that SWE proved valuable for the reclassification of low- and intermediate-suspicion nodules when employed in conjunction with ATA risk categories [17]. The findings of this study lend support to the hypothesis that future SWE-based risk stratification systems should explicitly account for nodule size, rather than relying on raw SWE values alone.

The Present Study Is Subject to a Number of Limitations

Firstly, the study was conducted in a single centre, and the sample size (100 patients, 343 nodules) was limited, particularly in certain subgroups (e.g., the single-nodule group, $n = 13$; the >20 mm size group, $n = 33$). The absence of a benign comparison nodule in the single-nodule group precluded calculation of specificity and AUC in that subgroup. In addition, the study population consisted of selected surgical patients with a high patient-level prevalence of malignancy (91%), which introduces potential spectrum bias; therefore, the predictive values reported here may not be generalisable to routine thyroid nodule assessment or to cytologically indeterminate nodules, in which the prevalence of malignancy is lower. Secondly, the measurements were performed under ex vivo conditions, and therefore do not directly reflect the impact of true intraoperative (in vivo) SWE application on clinical decision-making. The interruption of perfusion and possible changes in tissue tension in ex vivo tissue may cause SWE values to differ from in vivo measurements. Thirdly, the performance of SWE was not directly compared with frozen section on the same nodules in this study. Prospective studies performing this comparison will more definitively establish whether SWE is a genuine alternative to FS. Fourthly, SWE measurements were performed by a limited number of operators, and operator-dependent variability (e.g., pre-compression, ROI selection, scanning plane) is a recognised limitation of the technique [2]. A formal intra-observer/inter-observer agreement analysis was not performed in this study. Fifthly, the number of false-negative observations available for the GEE model was small ($n = 18$), and 17 of these occurred in nodules ≤ 10 mm; this resulted in a wide confidence interval for the tumour-size estimate, which should therefore be interpreted with caution, although sensitivity analyses confirmed the direction and statistical significance of this association. Finally, pathological tumour size and T-stage data were available for 91 patients, with these data missing for the remaining 9 patients. In addition, as lymph node dissection was not performed in any patient, the potential role of SWE in guiding the extension of surgery to the central compartment lymph nodes could not be evaluated; this warrants investigation in future prospective studies, building on previous ex vivo SWE work in level VI lymph nodes [18].

Notwithstanding these limitations, the nodule-based ex vivo design of the study and its GEE-based clustered analysis approach provide methodological strength in distinguishing the confounding effects of nodule number and tumour size.

5. Conclusions

It was demonstrated that shear wave elastography, when applied on a nodule-based basis ex vivo in thyroidectomy specimens, is capable of differentiating between benign and malignant thyroid nodules with a high degree of accuracy (AUC 0.94; sensitivity 84.2% and specificity 90.4% at the 25.40 kPa cutoff). The decrease in sensitivity observed at a fixed cutoff value as nodule number increases is a confounding effect arising from the relatively smaller size of malignant nodules in patients with multiple nodules, rather than from nodule multiplicity itself; no independent effect of nodule number was found once tumor size was controlled for. A robust positive correlation has been demonstrated between

tumour size and SWE stiffness value, with a concomitant significant reduction in SWE sensitivity observed in malignant nodules measuring 1 cm or less. The findings of this study indicate that ex vivo SWE, particularly when nodule size is considered, has the potential to serve as a valuable, rapid, and cost-effective adjunct or potential alternative to intraoperative frozen section in the assessment of thyroid malignancy. In order to validate this method, larger, multicentre, prospective studies are required. Such studies would need to evaluate the method under real-time in vivo conditions and in direct comparison with frozen section.

Author Contributions: Conceptualization, S.Ö.A., A.A.A. and I.B.A.; Visualization, I.B.A.; Data curation, M.G.D. and G.K.K.; Formal analysis, C.A., G.Y. and A.A.A.; Methodology, S.Ö.A. and G.Y.; Software, C.A. and G.K.K.; Supervision, M.G.D. and A.İ.S.; Writing—original draft preparation, S.Ö.A.; Writing—review and editing, A.İ.S. and S.Ö.A. All authors have read and agreed to the published version of the manuscript.

Funding: This research received no external funding.

Institutional Review Board Statement: This study was conducted in accordance with the Declaration of Helsinki and approved by the Non-Interventional Clinical Research Ethics Committee of Dokuz Eylül University Faculty of Medicine (Protocol No: 2024/13-05; Approval Date: 3 April 2024).

Informed Consent Statement: Patient consent was waived due to retrospective nature of this study and the use of anonymized data without any personal information.

Data Availability Statement: The datasets supporting the conclusions of this article are included within the article (and its additional files).

Conflicts of Interest: The authors declare no conflicts of interest.

Abbreviations

The following abbreviations are used in this manuscript:

FS	Frozen section
SWE	Shear-wave elastography
AUC	Area under the curve
ROI	Region of interest
SD	Standard deviation
ROC	Receiver operating characteristic
IQR	Interquartile range
kPa	Kilopascal
GEE	Generalized Estimating Equations
FNAB	Fine-needle aspiration biopsy
PPV	Positive predictive value
NPV	Negative predictive value
TI-RADS	Thyroid Imaging Reporting and Data System
ATA	American Thyroid Association
CI	Confidence interval

References

1. Kızılkaya, M.C.; Erözgen, F.; Akıncı, M.; Kaplan, R.; Tüzün, S.; Çıtlak, G. The predictive value of elastography in thyroid nodules and its comparison with fine-needle aspiration biopsy results. *Ulus. Cerrahi Derg.* **2014**, *30*, 147–152. [CrossRef] [PubMed]
2. Swan, K.Z.; Nielsen, V.E.; Bonnema, S.J. Evaluation of thyroid nodules by shear wave elastography: A review of current knowledge. *J. Endocrinol. Investig.* **2021**, *44*, 2043–2056. [CrossRef] [PubMed]
3. Goemann, I.M.; Paixão, F.; Migliavacca, A.; Guimarães, J.R.; Scheffel, R.S.; Maia, A.L. Intraoperative frozen section performance for thyroid cancer diagnosis. *Arch. Endocrinol. Metab.* **2022**, *66*, 50–57. [CrossRef] [PubMed]
4. Qiu, Y.; Xing, Z.; Yang, Q.; Luo, Y.; Ma, B. Diagnostic performance of shear wave elastography in thyroid nodules with indeterminate cytology: A systematic review and meta-analysis. *Heliyon* **2023**, *9*, e20654. [CrossRef] [PubMed]
5. Uludag, M.; Cetinoglu, I.; Unlu, M.T.; Kostek, M.; Caliskan, O.; Aygun, N. The role of frozen section examination in thyroid surgery. *Med. Bull. Sisli Etfal Hosp.* **2023**, *57*, 441–450. [CrossRef] [PubMed]

6. Gern, J.; Arbogast, M.; Alakus, H.; Brunner, S.; Schmidt, M.; Faust, M.; Bruns, C.J.; Schultheis, A.M.; Chiapponi, C. Intraoperative thyroid frozen section: Indications, results and consequences. *Gland Surg*. **2024**, *13*, 630–639. [CrossRef] [PubMed]
7. Jiang, C.; Chen, Y.; Zhang, C.; Jiang, B.; Qu, C.; Dong, G.; Wang, Y.; Wang, R.; Luo, Y.; Sang, J.; et al. Intraoperative frozen section for determining the extent of surgery in papillary thyroid carcinoma: Comprehensive risk factor assessment. *Gland Surg*. **2023**, *12*, 1705–1713. [CrossRef] [PubMed]
8. Ferraioli, G.; Barr, R.G.; Farrokh, A.; Radzina, M.; Cui, X.W.; Dong, Y.; Rocher, L.; Cantisani, V.; Polito, E.; D'Onofrio, M.; et al. How to perform shear wave elastography. Part I. *Med. Ultrason*. **2022**, *24*, 95–106. [CrossRef] [PubMed]
9. Ferraioli, G.; Barr, R.G.; Farrokh, A.; Radzina, M.; Cui, X.W.; Dong, Y.; Rocher, L.; Cantisani, V.; Polito, E.; D'Onofrio, M.; et al. How to perform shear wave elastography. Part II. *Med. Ultrason*. **2022**, *24*, 196–210. [CrossRef] [PubMed]
10. Cakir, B.; Aydin, C.; Korukluoğlu, B.; Ozdemir, D.; Sisman, I.C.; Tüzün, D.; Oguz, A.; Güler, G.; Güney, G.; Kuşdemir, A.; et al. Diagnostic value of elastosonographically determined strain index in the differential diagnosis of benign and malignant thyroid nodules. *Endocrine* **2011**, *39*, 89–98. [CrossRef] [PubMed]
11. Bender, Ö.; Kılıç, Y.; Hot, S.; Ertürk, A.; Coşkun, Z.Ü.; Akan, A. Diagnostic accuracy and reliability of ultrasound elastography in the evaluation of thyroid nodules. *Okmeydanı Tıp Derg*. **2012**, *28*, 151–156. [CrossRef]
12. Naleini, F.; Pirani, A.; Naseri, R.; Karami, Z.; Rashidi Shahpasandi, M.H.; Bahrami Kamangar, P.; Bakhtiari, N. Comparing shear wave elastography and fine needle aspiration in the diagnosis of solid thyroid nodules. *Eur. J. Transl. Myol*. **2022**, *32*, 10635. [CrossRef] [PubMed]
13. Nattabi, H.A.; Sharif, N.M.; Yahya, N.; Ahmad, R.; Mohamad, M.; Zaki, F.M.; Yusoff, A.N. Is diagnostic performance of quantitative 2D-shear wave elastography optimal for clinical classification of benign and malignant thyroid nodules?: A systematic review and meta-analysis. *Acad. Radiol*. **2017**, *in press*. [PubMed]
14. Zhang, Y.X.; Xue, J.P.; Li, H.Z.; Miao, J.W.; Kang, C.S. Clinical value of shear wave elastography color scores in classifying thyroid nodules. *Int. J. Gen. Med*. **2021**, *14*, 8007–8018. [CrossRef] [PubMed]
15. Chambara, N.; Lo, X.; Chow, T.C.M.; Lai, C.M.S.; Liu, S.Y.W.; Ying, M. Combined shear wave elastography and EU TIRADS in differentiating malignant and benign thyroid nodules. *Cancers* **2022**, *14*, 5521. [CrossRef] [PubMed]
16. Petersen, M.; Schenke, S.A.; Firla, J.; Croner, R.S.; Kreissl, M.C. Shear wave elastography and thyroid imaging reporting and data system (TIRADS) for the risk stratification of thyroid nodules—Results of a prospective study. *Diagnostics* **2022**, *12*, 109. [CrossRef] [PubMed]
17. Gao, L.; Xi, X.; Jiang, Y.; Gao, Q.; Tang, J.; Yang, X.; Zhu, S.; Zhao, R.; Lai, X.; Zhang, B. Prospective differentiation of difficult-to-diagnose thyroid nodules using shear wave elastography. *J. Cancer Res. Ther*. **2025**, *21*, 1115–1120. [CrossRef] [PubMed]
18. Chang, W.; Tang, L.; Lu, C.; Wu, M.; Chen, M. Shear wave elastography in the evaluation of level VI lymph nodes in papillary thyroid carcinoma: Combined with gray-scale ultrasound ex vivo. *BMC Cancer* **2018**, *18*, 1001. [CrossRef] [PubMed]
19. Haugen, B.R.; Alexander, E.K.; Bible, K.C.; Doherty, G.M.; Mandel, S.J.; Nikiforov, Y.E.; Pacini, F.; Randolph, G.W.; Sawka, A.M.; Schlumberger, M.; et al. 2015 American Thyroid Association management guidelines for adult patients with thyroid nodules and differentiated thyroid cancer: The American Thyroid Association Guidelines Task Force on Thyroid Nodules and Differentiated Thyroid Cancer. *Thyroid* **2016**, *26*, 1–133. [CrossRef] [PubMed]

Disclaimer/Publisher's Note: The statements, opinions and data contained in all publications are solely those of the individual author(s) and contributor(s) and not of MDPI and/or the editor(s). MDPI and/or the editor(s) disclaim responsibility for any injury to people or property resulting from any ideas, methods, instructions or products referred to in the content.